Scanning Electron Microscopy

Volume 3
Number 1 *3rd Pfefferkorn Conference*

Article 25

1984

A Computer Controlled Scanning Transmission Electron Microscope Equipped with an Energy Analyzer for Special Investigations on Electron Diffraction- and Channeling Patterns

W. Hylla
Optisches Institut der Technischen Universitat Berlin

H.-J. Kohl
Optisches Institut der Technischen Universitat Berlin

H. Niedrig
Optisches Institut der Technischen Universitat Berlin

D. Wendtland
Optisches Institut der Technischen Universitat Berlin

Electron Optical Systems (pp. 237-244)
SEM Inc., AMF O'Hare (Chicago), IL 60666-0507, U.S.A.

0-931288-34-7/84$1.00+.05

A COMPUTER CONTROLLED SCANNING TRANSMISSION ELECTRON MICROSCOPE EQUIPPED WITH AN ENERGY ANALYZER FOR SPECIAL INVESTIGATIONS ON ELECTRON DIFFRACTION- AND CHANNELING PATTERNS

W. Hylla, H.-J. Kohl, H. Niedrig, D. Wendtland

Optisches Institut der Technischen Universitat Berlin
Sekretariat P 11
Strasse des 17. Juni 135
D-1000 Berlin - 12
W. Germany

Abstract

A scanning electron microscope was equipped with a double tilting stage, driven by stepping motors, to investigate electron channeling patterns (ECPs) and large angle convergent beam patterns (LACBPs) of single crystals. Transmitted electrons may be energy-selected by a magnetic sector-field energy analyzer. The recording of experimental data and the experimental arrangement are controlled by a microprocessor system, including a picture storage unit of 512 x 512 pixels of 16 bit. Recorded patterns can be stored on 1 Megabyte floppies.

A set of useful programs allows one to perform calculations with stored patterns, e.g., contrast enhancement or -inversion, noise reduction, difference or quotient of two patterns etc. The possibility of background subtraction (e.g., in patterns recorded with characteristic energy loss electrons) allows one to get true K-loss convergent beam patterns. Other recording modes allow one to get two CBPs simultaneously recorded with electrons of different energy losses, to measure angle dependences of energy selected electrons, or to take electron energy loss spectra.

A special processor program generates a theoretically calculated CBP or ECP on the TV screen and prints out a list of all band edges up to a chosen limit of Miller indices (hkl). The program requires the coordinates of two known poles and some crystallographic properties of the investigated material. Thus complete indexing of recorded diffraction patterns is easily possible.

The system has been applied, e.g., to investigate localization effects of electron Bloch-waves in graphite.

Key Words: Convergent beam patterns; crystal orientation, digital image recording, electron channeling patterns, electron diffraction, electron energy loss spectroscopy, inelastic scattering, rocking-crystal.

Address for correspondence:
H. Niedrig, Optisches Institut der TU Berlin
Strasse des 17. Juni 135, D-1000 Berlin - 12
W. Germany
Phone No.: 030 - 314 2735

Experimental Set-up

Electron Optics

An electron optical arrangement has been built up, which offers some very special possibilities of investigations on electron scattering processes. The column consists mainly of the probe forming system (tungsten cathode, double condenser, final lens with scan-coils inside), a double-tilting stage for backscattering and transmission, driven by stepping motors, and an energy-selecting double focussing magnetic sector-field analyzer /2/.

Tilting-stage

The specimen is mounted on a stage in a Cardanic suspension, which permits tilting of $\pm$ 20° in both axes. Additional stepping motors for sample shift and the possibility of mechanical shift of the whole assembly allow a) to adjust the selected specimen area into the pivot point of the tilting-stage, and b) to adjust the pivot point into the electron optical axis. Two secondary electron detectors of Everhart-Thornley type and a surface barrier semiconductor ring detector are mounted above the specimen. Below the ground plate, a second semiconductor ring detector collects transmitted electrons, scattered into angles greater than $\approx$ 20 mrad (dark field detector). A magnetic sector-field energy analyzer with a maximum acceptance angle of 2α = 60 mrad provides the energy distribution of the transmitted electrons, or allows to get energy-selected transmission diffraction patterns /4/.

Microprocessor control

The stepping motors for the tilting movement of the specimen and the magnetic coil current of the energy analyzer are controlled by a microprocessor system (Z 80 based), which also manages data acquisition /3/. Accessing to a 256 kbyte memory, video pictures containing 512 x 512 pixels of 16 bit (65,536 grey levels) can be stored and read out with normal TV frequency. Permanent storage is possible on 1 Mbyte floppies with a transfer time of around 50 seconds. The processor was programmed to perform several calculations using an implemented APU (arithmetic processing unit). Offset subtraction, optimum contrast expansion, noise reduction by averaging, difference- or quotient - patterns and so on can be performed quickly (calculation times up to 3 min.). The set-up in principle is shown in fig. 1.

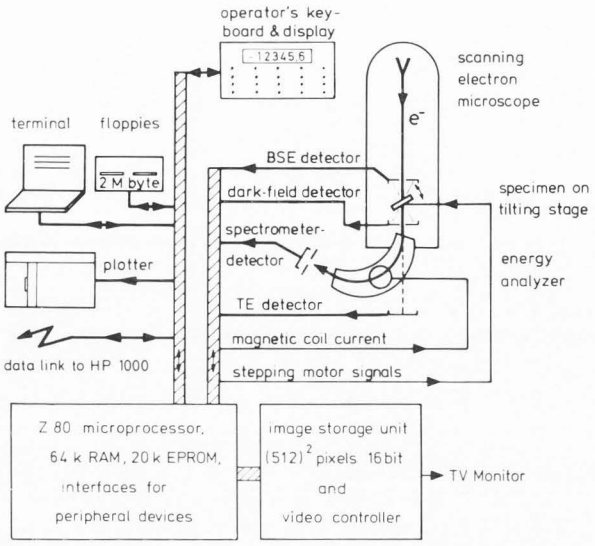

Fig.1: Experimental set-up for computer-controlled recording of energy-selected electron diffraction patterns.

Energy-selected Convergent-Beam-Patterns (CBPs)

Recording modes and some examples

Generally, three different kinds of recordings can be performed under control of the microprocessor: 1) Rocking-curves (linescans) are obtained by tilting the crystal in one axis (see fig. 2). 2) Diffraction patterns are obtained by rocking the crystal sequently in both axes: Electron Channeling Patterns, using the backscatter detector, Large-Angle-Convergent-Beam Patterns, using the transmission detector (see fig. 3 a,b). 3) Energy-loss spectra of transmitted electrons are obtained by ramping the magnet-coil current of the energy-analyzer (see fig. 4 a,b,c). By suitable programming of the microprocessor, some very special investigations become possible, e.g.: simultaneous recording of two energy-selected convergent-beam-patterns at different energies; creating pictures of energy-selected rocking-curves, lying one upon another, recorded with increasing energy-loss ΔE, thus showing the dependence of different energy losses on the diffraction contrast in a rocking-curve.

Comparison of two energy-selected LACBPs, recorded at different energy-losses

The simultaneous recording of two LACBPs at different energy losses is managed by the processor by switching the energy-analyzer for each increment of tilt between the two preselected energies. In this way, the two recorded patterns become directly comparable as they are not affected (or both in the same way) by long time effects like contamination or intensity drifts etc. That is important if it is intended to do quantitative calculations with the two patterns. The example, given below (fig. 6) points out the differences in two LACBPs, the first taken with electrons of the multiple scattering background, and the other with electrons which have suffered a characteristic

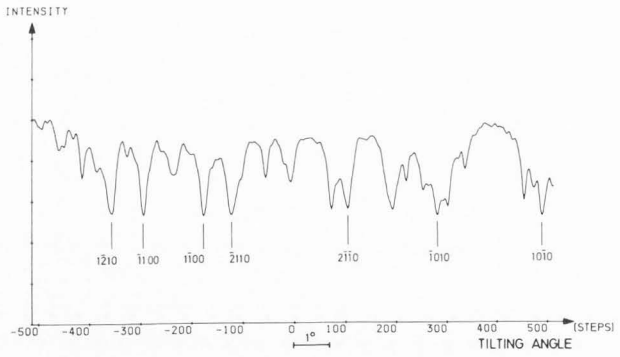

Fig.2: Rocking-curve (linescan) through a graphite large angle convergent beam pattern near the 001-pole. Band edges of low order are marked with their Miller indices.

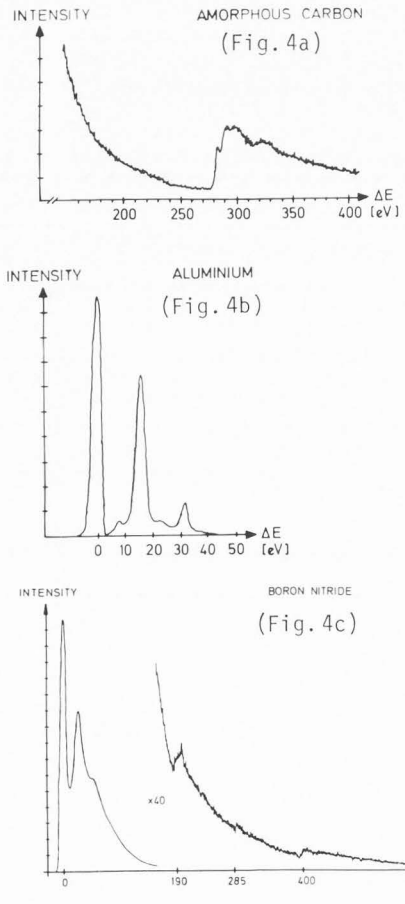

Fig.4: Three examples of electron energy loss spectra:
a) Carbon K-loss of an evaporated thin film (E_o = 20keV)
b) Aluminium plasmon losses of a polycrystalline film (E_o = 20keV)
c) Spectrum of tapered Boron Nitride (E_o = 30keV).

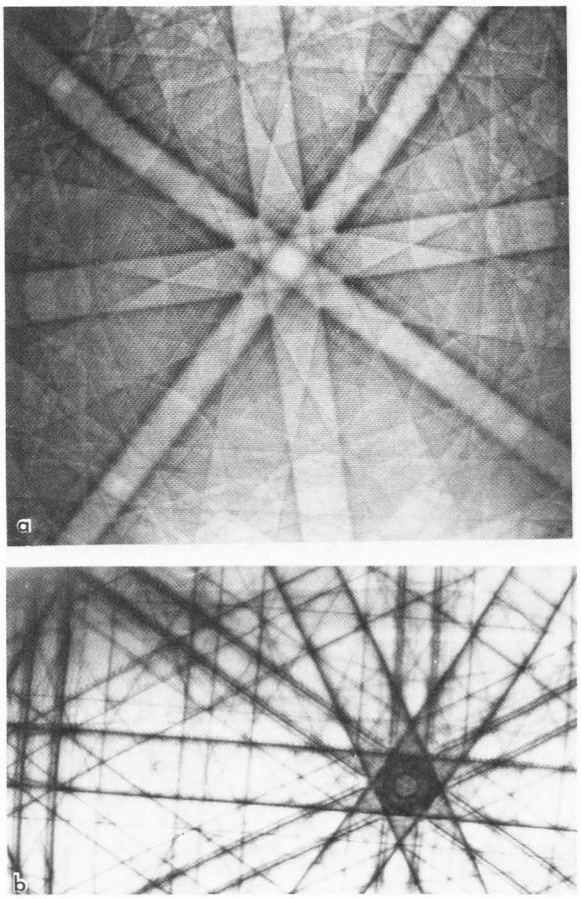

Fig.3: Electron diffraction patterns obtained through the rocking-crystal method:
a) Electron channeling pattern of 100-orientated Germanium (28°x28°, E_0 = 40keV)
b) Large angle convergent beam pattern of graphite (28°x14°, E_0 = 40keV).

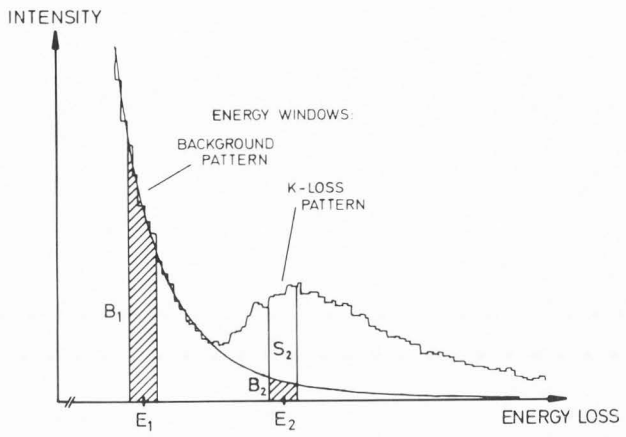

Fig.5: Computer performed backround-fitting and subtraction for recording of true characteristic energy loss patterns. The background pattern at E_1 and the K-loss pattern at E_2 are recorded simultaneously.

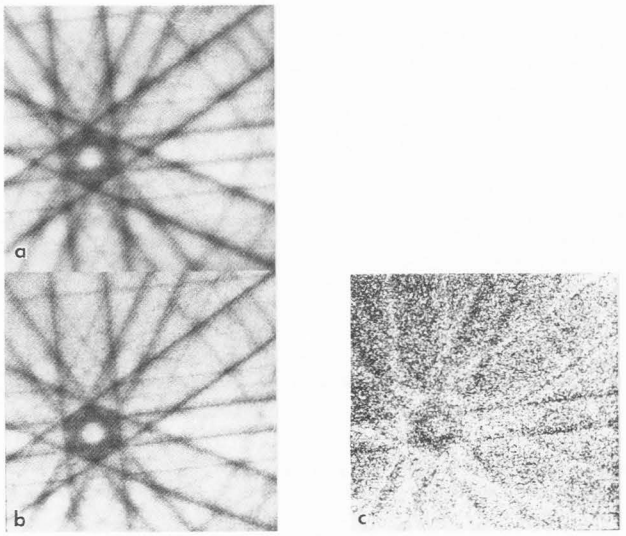

Fig.6: Comparison of energy-selected LACBPs of graphite:
a) Background pattern recorded around 50eV below K-loss energy
b) K-loss pattern (background stripped) recorded simultaneously with a) at 15eV above K-loss energy
c) Difference pattern of the equalized patterns a) and b).

energy-loss. To obtain a true characteristic energy-loss pattern, it is necessary to subtract the background, due to multiple scattering processes. This is done as follows:

- Processor performed background fitting, using the inverse power law $I = A \cdot (E-Eo)^{-r}$ with I: Intensity, E: Energy loss, Eo: Energy offset; A, r: fitting parameters. This formula is slightly modified, compared to that in common use /7/.
- Calculation of the ratio B_1/B_2 from the spectrum (see fig. 5)
- Taking the intensity of a pattern pixel, recorded at E_1 and calculating the corresponding B_2, using B_1/B_2.
- Subtracting the calculated B_2 from the pixel intensity, recorded at E_2.

This procedure is performed for all of the 131,000 pixels of the characteristic loss pattern. The only assumption of this procedure is, that the shape of the multiple scattering background remains always the same, independent of the angle of incidence of the primary electrons. To minimize the error due to long time effects (such as increasing background caused by contamination of hydrocarbons) a new spectrum is recorded and stored at the end of each rocking-curve, i.e. each line of the picture. Fig. 6 shows two LACBPs of a graphite crystal, taken simultaneously in that way, the K-loss pattern background stripped /6/. For direct comparison, both patterns were pushed to the same value of mean intensity and then a difference pattern

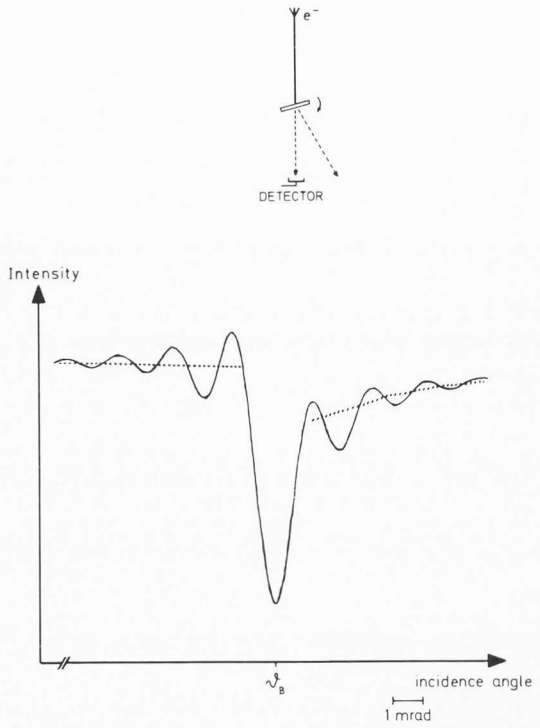

Fig.7: Two-beam approximation of K-loss intensity in a rocking-curve of graphite in the region of $01\bar{1}0$ Bragg reflection.

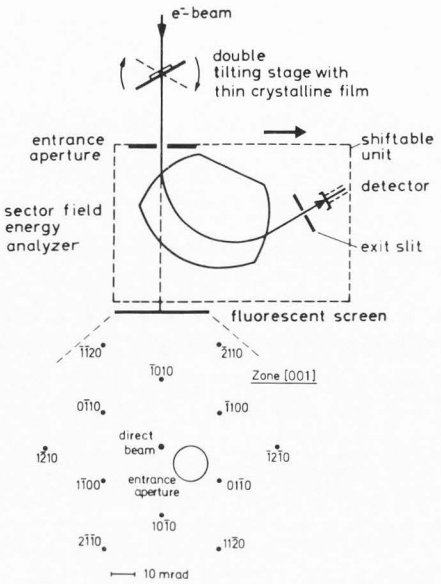

Fig.8: Diagrammatic sketch of the shiftable energy analyzer and enlargement of the graphite diffraction pattern in correct scale. The position of the entrance aperture to record fig.9c is marked.

"K-loss picture minus background picture" was calculated (fig. 6 c). This pattern clearly points out some differences of K-loss and background pattern: a) the dark band edges occur even in the difference pattern; that means a slightly higher diffraction contrast is present in the K-loss pattern. That can be understood, considering that electrons, contributing to the K-loss pattern, suffered only one scattering process, whereas electrons of the diffuse background were scattered several times, causing a loss of information of the elastic intensity distribution (diffraction contrast); b) the dark lines seem to be hemmed in by light seams, pointing out, that the dark lines (band edges) in the background pattern are slightly broader than those in the K-loss pattern. That also may be an effect of multiple scattering of the background electrons: The electron beam is broadened by repeated scattering which occurs as a softening of the Bragg condition.

Visualization of the localization effect in light elements

The experimental set-up of the energy analyzer provides a lot of freedom in adjusting the system in respect to the electron optical axis. Shifting of the whole analyzer assembly allows one to collect electrons which are scattered off the direct beam. The maximum scattering angle which can be accepted by an entrance aperture of 2α = 10 mrad is 30 mrad out of the direct beam. That can be used to emphasize the localization effect of Bloch-waves in light elements such as graphite. Localization effect of Bloch-waves means, that for angles of incidence deviating a small amount from the exact Bragg angle, the Bloch-waves arising under the periodic potential of the crystal are concentrated with their maxima of probability amplitude on or between the atomic sites, respectively. That leads to an asymmetry in intensity of rocking-curves through CBPs in the region of band edges (fig. 7). For the crystal thicknesses, used in our experiments ($t \approx$ 100...300 nm) the superimposed elastic diffraction contrast covers this weak effect, so that an additional suppression of diffraction contrast seems to be appropriate /8/.

This can be done for one selected band edge by shifting the entrance aperture of the energy-analyzer half the way between direct beam and the Bragg reflection corresponding to the band edge to be suppressed. Then, because of the symmetric position between direct beam and Bragg-reflection, the same amounts of scattering reach the shifted entrance aperture, no matter whether the main part of intensity is in the direct beam or in the Bragg-reflection, thus leading to elimination of diffraction contrast for this band edge.

As an example, we chose the $(01\bar{1}0)$ band edge of a graphite LACBP to be suppressed. Fig. 8 shows the position and the acceptance angle of the entrance aperture, which can be adjusted by watching the diffraction pattern on a fluorescent screen below the analyzer with magnet coil current switched off. This figure shows the real proportions on the screen at 40 keV primary energy. Fig. 9 demonstrates the resulting changes in the K-loss LACBP. Fig. 9a shows the zero-loss pattern recorded in the direct beam, for indexing and comparison. In figs. 9b, c, the background-stripped K-loss patterns, recorded in the direct beam and with shifted entrance aperture, respectively, are compared. The pattern in fig. 9c

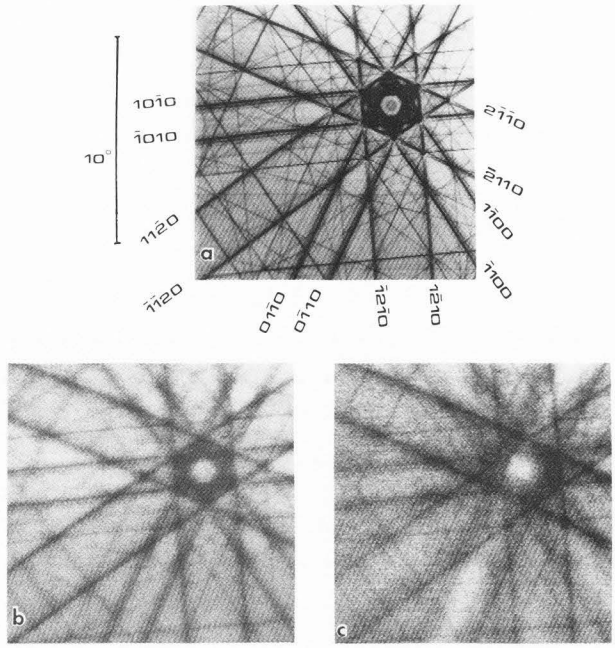

Fig. 9: Visualization of Bloch-wave localization effect:
a) Zero-loss LACBP (graphite, E_0 = 40keV), band edges of lowest indices are given
b) K-loss pattern (background stripped) recorded in the direct beam
c) K-loss pattern (background stripped) recorded with detector aperture shifted half the way between direct beam and $01\bar{1}0$ reflection.

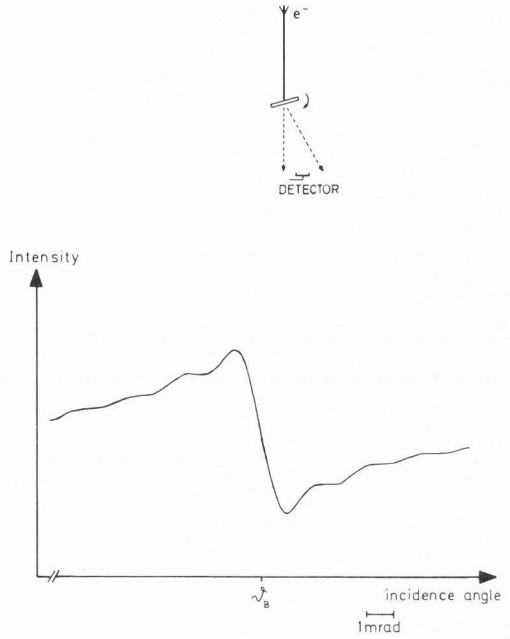

Fig.10: Two-beam approximation of K-loss intensity in a rocking-curve of graphite in the region of $01\bar{1}0$ Bragg angle, detector shifted between direct beam and Bragg reflection.

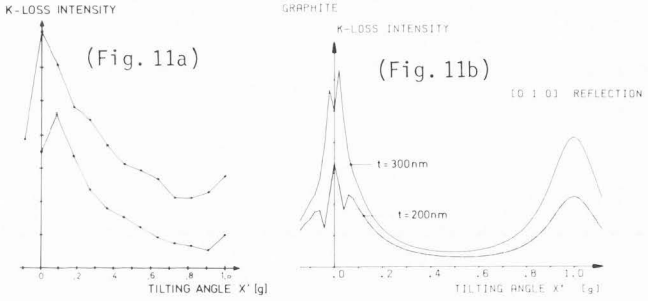

Fig.11: Angle dependence of Carbon K-loss electrons:
a) experimental results obtained for two different film thicknesses
b) two-beam approximation for 200nm and 300nm film thickness.

clearly points out the predicted effects: 1.- the sharp ($01\bar{1}0$) band edge, representing the diffraction contrast, has vanished, 2.- a remarkable asymmetry in the region of the suppressed band edge arose. That indicates the stronger scattering for incidence angles smaller than Bragg angle, corresponding to the excitation of mainly the strongly absorbed type II Bloch-waves with their maxima of probability amplitude just on the atomic sites. The predominant occurrence of the weakly absorbed type I Bloch-waves for incidence angles somewhat larger than Bragg angle, causes a region of decreased intensity outside the vanished band edge in fig. 9c. That experimental result is in good agreement with a two-beam calculation shown in fig. 10, based on Bethe cross-sections for K-shell ionization of carbon /1/, /5/.

This mode of recording may be of further interest for investigations on the crystal structures, the atomic sites or the inelastic scattering cross-sections of di- or poly-atomic crystals /11/.

Measurements of angle dependence of inelastically scattered electrons

The possibility of shifting the energy-analyzer in respect to the electron optical axis allows one to investigate angular distributions of inelastically scattered electrons, e.g., those which suffered a characteristic energy loss through inner shell ionization. Similar measurements have been carried out for aluminium and silicon by Oikawa et al. /10/. We made first measurements on thin graphite crystals, tilted to a Bragg position, so that nearly a two-beam case was realized. The angular dependence of the K-loss signal in the energy range from 295 up to 305 eV is shown in fig. 11a for two different film thicknesses. The site of maximum intensity is very sensitive with respect to the film thickness, because it is an effect of the subsidiary lines. This is also stated in calculated two-beam approximations which are given in fig. 11b. These results differ on principle from those of Oikawa et al. /10/, who found, that Bragg-reflected electrons do not excite inner-shell electrons, contrary to our measurements. For clarifying the problem, further measurements have to be carried out.

Processor program for complete indexing of channeling- and convergent-beam-patterns

The program ORIENT

Because in the majority of experiments we use single crystalline materials, we developed a simple computer program, written in FORTRAN IV, which allows complete indexing of channeling- and convergent-beam-patterns. This program is based on the geometrical conditions for Bragg reflection, and the main input data are: - coordinates of two known poles (e.g. taken from an experimentally obtained pattern), - dimensions of the crystal unit cell, - relative sites of the atoms in the unit cell, - covered angle range of the pattern to be generated, - primary electron energy, - number of band edges and lowest (hkl) may be selected, - all included poles or only poles of a certain type may be marked.

The program starts with the set of lowest allowed (hkl) and checks, if Bragg condition is fullfilled for any two points on the margin of the pattern. In this case, the related band edge (hkl) crosses the pattern, and the program runs in 512 steps through the total range of one tilting angle, calculating for each angle-coordinate the corresponding other one, which satisfies the Bragg condition. All pairs of coordinates found this way, representing the band edge (hkl), are set to a white (or dark) level in the image memory. The equations for calculation of the incidence angle between electron beam and tilted crystal coordinates are matched to the constructional realities of the Cardanic suspension of the double-tilting stage, leading to an according high conformity between experimental and calculated patterns.

As an example, fig. 12 shows an experimentally obtained LACBP of graphite, in comparison with a superposition of the calculated pattern. With the aid of the computer output, (fig. 13) every band edge can easily be identified, looking for its intersections with the margin of the pattern, and finding these tilting-step coordinates out of the given listing.

Orientation determination with the aid of ORIENT

We applied this possibility of complete determination of crystal orientation for realization of special investigations of anisotropic emission of atoms under ion bombardment /9/. For these investigations, it was necessary to cut a slice of single crystalline material out of a crystalline rod /12/ with a surface normal to the [11 3 1] direction. To determine the required tilting angles of the goniometric stage of the cutting device, a large angle ECP simulation with the same orientation as the face of the crystalline rod was calculated, and the angle coordinates of all [11 3 1] poles were printed out (fig. 14a). Then the goniometric stage was tilted by exactly these amounts which lead to an [11 3 1] pole, and a slice was cut out. The ECP we got from this slice is shown in fig. 14b. The [11 3 1] poles are marked, and we found the central one to deviate around 2.9° from the surface normal. These faults depend on the precision in adjusting the crystal on the tilting-stage, that means a) alignment of a marked direction on the crystal surface parallel to one tilting axis b) adjusting the surface normal parallel to the electron optical axis for zero-tilt position. We estimate that these faults can be minimized to less than ± 1° in total.

Input poles:

1. U V W = 1 1 2 X, Y = -266., -154. steps
2. U V W = 0 1 2 X, Y = 410., 172. steps

Pattern tilting range:

degrees: (X: -7.1 to 7.0) * (Y: -7.1 to 7.0)
steps: (X: -512. to 510.) * (Y: -512. to 510.)

Listing of drawn band edges:

H	K	I	L	X-Y-Bragg (steps) 1.intersect.pt. with pattern margins		2.intersect.pt.		width (deg)	relative intensity
0	1	-1	0	-259.	510.	-512.	388.	1.62	.340
1	0	-1	0	-187.	510.	510.	30.	1.62	.340
-1	0	1	0	21.	510.	510.	174.	1.62	.340
1	-1	0	0	-348.	-512.	-277.	510.	1.62	.340
-1	1	0	0	-230.	-512.	-159.	510.	1.62	.340
0	-1	1	1	285.	-512.	510.	-405.	1.70	.554
1	1	-2	0	-392.	510.	510.	439.	2.80	.508
1	-2	1	0	-394.	510.	-512.	336.	2.80	.508
-1	2	-1	0	-148.	510.	-512.	-31.	2.80	.508
2	-1	-1	0	209.	-512.	-282.	510.	2.80	.508
-2	1	1	0	433.	-512.	-56.	510.	2.80	.508
0	2	-2	0	-123.	510.	-512.	322.	3.23	.086
2	0	-2	0	-290.	510.	510.	-42.	3.23	.086
-2	0	2	0	125.	510.	510.	245.	3.23	.086
2	-2	0	0	-406.	-512.	-335.	510.	3.23	.086
-2	2	0	0	-172.	-512.	-100.	510.	3.23	.086
0	-2	2	1	-512.	-141.	510.	354.	3.28	.143
0	2	-2	-1	-512.	-407.	510.	88.	3.28	.143
2	-2	0	1	226.	-512.	319.	510.	3.28	.143
-2	2	0	-1	464.	-512.	510.	-35.	3.28	.143
-2	0	2	1	492.	-512.	-512.	155.	3.28	.143
2	0	-2	-1	63.	-512.	-512.	-133.	3.28	.143
0	-2	2	2	141.	-512.	510.	-336.	3.39	.074

Poles:

U	V	W	P	Q	R	S	X, Y (steps)	
0	1	2	-1	2	-1	6	410.	172.
1	1	2	1	1	-2	6	-266.	-154.
1	2	4	0	1	-1	4	72.	9.

Fig.13: Computer output for identification and indexing of poles and band edges.

Summary

An electron optical device has been built up, which allows by means of a Z 80 microprocessor system some special investigations on electron scattering and diffraction processes. Energy-selected Large-Angle-Convergent-Beam-Patterns were taken and compared one to another. A method for visualization of localization contrast in light elements was pointed out. Angular distributions of inelastically scattered electrons were measured. ECPs and LACBPs were used to get a complete determination of crystal orientation. This was done by applying a developed microprocessor program.

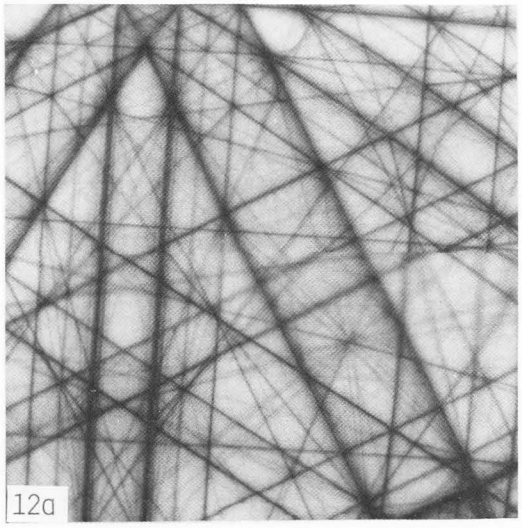

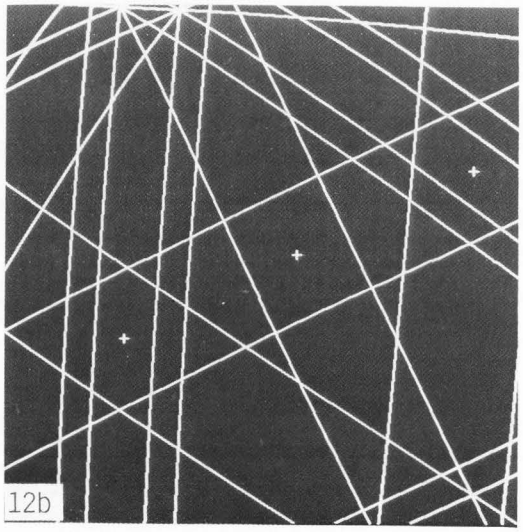

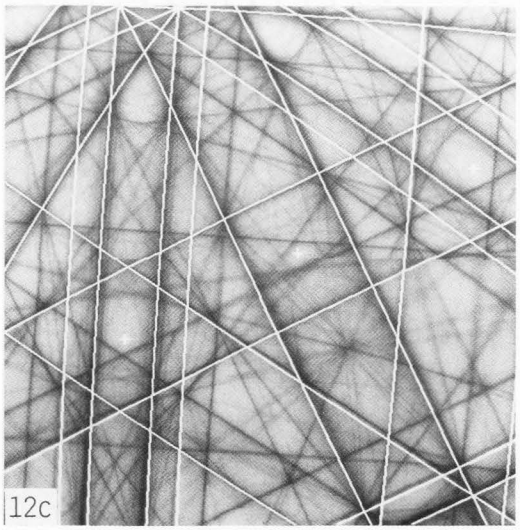

Fig.12: Comparison of experimentally obtained and computer generated diffraction patterns:
a) LACBP of graphite near 001 pole
b) computer simulation of the 23 lowest indexed band edges
c) overlay of both patterns in the image storage unit.

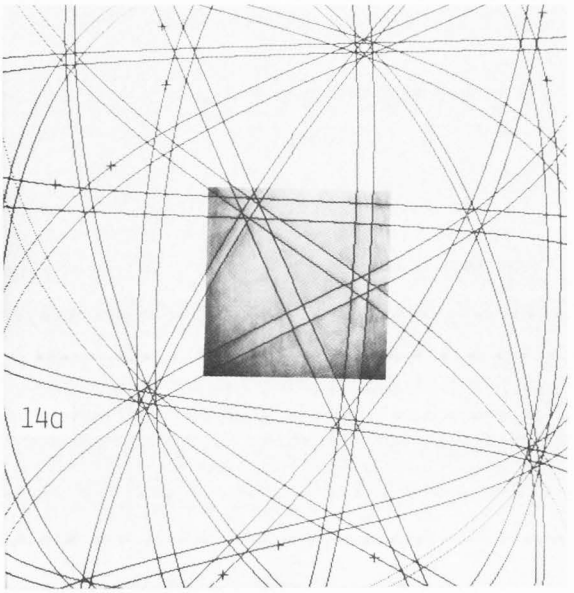

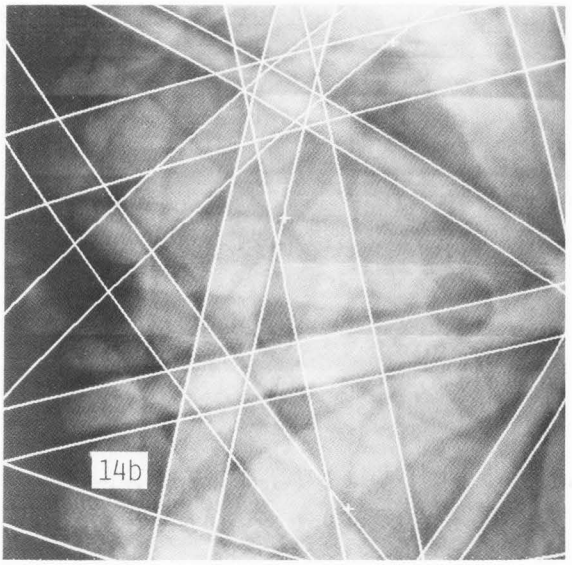

Fig.14: Application of orientation determination:
a) experimentally obtained ECP of a silver rod (central field, 14°x14°), overlaid with a large angle simulation in the same orientation to get the angle coordinates of poles of [11 3 1]- type (marked)
b) ECP of a silver slice cut with a surface normal nearly parallel to the [11 3 1] direction. The central pole (white cross) deviates 2.9° from surface normal.

Acknowledgements

This work has been supported by grants of the "Deutsche Forschungsgemeinschaft".

References

/1/ Bethe H. (1930). Zur Theorie des Durchgangs schneller Korpuskularstrahlen durch Materie. Ann. Phys. 5, 325-400

/2/ Brunner M. (1981). Rocking Crystal Electron Channeling Patterns, Backscattering and Transmission. Scanning Electron Microscopy 1981; I: 385-396

/3/ Brunner M, Burchard D, Hylla W, Kohl H-J, Niedrig H, Wendtland D. (1982). A Digital Storage Unit Combined With an Electron Microscope for Recording Comparable ECPs Obtained With Different Signals. 10th Intern. Congr. Electr. Microsc., Hamburg, Germany (West), JP LePoole et al. (ed.), (Dtsche. Ges. f. Elektr. Mikr., Frankfurt, W. Germany), I: 443-444

/4/ Brunner M, Hylla W, Kohl H-J, Niedrig H, Wendtland D. (1983). Electron Channeling Contrast in Characteristic Energy-Loss Intensity Investigated By the Rocking-Crystal Method. Scanning Electron Microsc. 1983; I: 99-104

/5/ Egerton RF. (1979). K-Shell Ionization Cross-Section for Use in Microanalysis. Ultramicroscopy, 4, 169-179

/6/ Hylla W, Kohl H-J, Niedrig H, Wendtland D. (1983). Direct Observation of Bloch-Wave Localization Effect in Light Elements by Suitable Detector Arrangement. Beitr. elektronenmikroskop. Direktabb. Oberfl. 16, G Pfefferkorn (ed.), Verlag R.A. Remy, Muenster, Germany (West), 67-74

/7/ Joy DC, Maher DM. (1979). 'The Basic Principles of EELS' and 'Elemental Analysis Using Inner Shell Excitations' in: Introduction to Analytical Electron Microscopy, J. Hren et al. (ed.), Plenum Press, N.Y., 223-244 and 259-294

/8/ Kohl H-J. (1983). A Matrix Formulation of the Inelastic Scattering of Electrons in Crystals. Beitr. elektronenmikroskop. Direktabb. Oberfl. 16, G Pfefferkorn (ed.), Verlag R.A. Remy, Muenster, Germany (West), 75-80

/9/ Linders J, Niedrig H, Sternberg M. (1984). Undistorted Measurements of Differential Sputtering Yields Using the Collector Method by Means of Electron Backscattering. Proc. 10th Int. Conf. Atomic Collisions in Solids, Bad Iburg, Germany (West), publ. in: Nucl. Instr. Meth. Phys. Res. (North Holland, Amsterdam), B2: 649-654

/10/ Oikawa T, Hosoi J, Inoue M, Honda T. (1984). Scattering Angle Dependence of Signal/Background Ratio of Inner Shell Electron Excitation Loss in EELS. Ultramicroscopy, 12, 223-230

/11/ Spence JCH, Taftø J. (1982). Atomic Site and Species Determination Using the Channeling Effect in Electron Diffraction. Scanning Electron Microscopy 1982; II: 523-531

/12/ Whitton JL, Carter G. (1980). The Development of Surface Topography by Heavy Ion Sputtering, Perchtoldsdorf, Austria, P Varga et al. (ed.), Inst. f. Allg. Phys., TU Wien, 552-572